

# Performance study of 40-Gb/s RZ signals through cascaded thin-film filters with large dispersion slope

Yue Wang<sup>1</sup>, Weisheng Hu<sup>1</sup>, Yikai Su<sup>1</sup>, Zheng Zheng<sup>2</sup>, Lufeng Leng<sup>3</sup>, Xiangqing Tian<sup>1</sup>, and Yaohui Jin<sup>1</sup>

1. State Key Laboratory of Advanced Optical Communication Systems and Networks, Shanghai Jiao Tong University, Shanghai, 200030, China.

[wangyue@sjtu.edu.cn](mailto:wangyue@sjtu.edu.cn); [wshu@sjtu.edu.cn](mailto:wshu@sjtu.edu.cn)

2. School of Electrical and Information Engineering, Beihang University, Beijing, 100083, China.

3. New York City College of Technology, City University of New York, 300 Jay Street, Brooklyn, NY 11201, USA.

**Abstract:** The performance of 40-Gb/s RZ signals through cascaded thin-film filters is investigated by both numerical and analytical means. It is observed that the filtering effects can reduce the eye closure penalties caused by the large dispersion slope of the thin-film filters. In addition, the performance can be further improved by proper frequency detuning between the signal and the center of the filter. The combined effects of dispersion slope and filtering on 40-Gb/s signals are investigated analytically and explained for typical bit patterns.

©2005 Optical society of America

OCIS codes: (060.4510) Optical communications; (120.2440) Filters; (260.2030) Dispersion

---

## References and links

1. Robert B. Sargent, "Recent advances in thin film filters," in *Proc. Optical Fiber Communication Conference* (Optical Society of America, Los Angeles, CA, 2004), paper TUD6.
2. G. Lenz, B. J. Eggleton, C. R. Giles, C. K. Madsen, and R. E. Slusher, "Dispersive properties of optical filters for WDM systems," *IEEE J. Quantum Electron.* **34**, 1390-1402 (1998).
3. Ioannis Zacharopoulos, Anna Tzanakaki, D. Parcharidou, and I. Tomkos, "Improved filter concatenation tolerance using duobinary modulation format for metropolitan area networks," in *IEEE-LEOS Annu. Meeting* (IEEE Lasers and Electro-Optics Society, Tucson, Arizona, 2003), paper WY2, pp. 680-681.
4. Mark Kuznetsov, Nan M. Froberg, Scott R. Henion, and Kristin A. Rauschenbach, "Power penalty for optical signals due to dispersion slope in WDM filter cascades," *IEEE Photon. Technol. Lett.* **11**, 1411-1413 (1999).
5. G. Lens and L.E. Adams, "Dispersion and crosstalk of optical minimum phase filters in wavelength division multiplexed systems," in *Proc. Optical Fiber Communication Conference/ International Conference on Integrated Optics and Optical Fiber Communication* (Optical Society of America, San Diego, Calif., 1999), paper WJ5, pp. 168 -170.
6. Ioannis Tomkos, June-Koo Rhee, Pakir Iydrroose, Robert Hesse, Aleksandra Boskovic, and Rich Vodhanel, "Filter concatenation penalties for 10-Gb/s chirped transmitters suitable for WDM metropolitan area networks," *IEEE Photon. Technol. Lett.* **14**, 564-566 (2002).
7. John D. Downie, Frank Annunziata and Jason Hurley, "Fixed low-channel-count optical ADD-DROP multiplexer filter concatenation experiments with 50-GHz channel spacing and 10-Gbit/s NRZ signals," *J. Opt. Netw.* **3**, 204-213, (2004), <http://www.osa-jon.org/abstract.cfm?URI=JON-3-4-204>.
8. Mark Jablonski, Yuichi Takushima and Kazuro Kikuchi, "The realization of all-pass filters for third-order dispersion compensation in ultrafast optical fiber transmission systems," *IEEE J. Lightwave Technol.* **19**, 1194-1205 (2001).
9. João L. Rebola and Adolfo V. T. Cartaxo, "Power penalty assessment in optically preamplified receivers with arbitrary optical filtering and signal-dependent noise dominance," *J. Lightwave Technol.* **20**, 401-408 (2002).
10. T. Tökle, C. Peucheret, P. Jeppesen, "Advanced modulation formats in 40 Gb/s optical communication systems with 80km fibre spans," *Opt. Commun.* **225**, 79-87 (2003).
11. Govind P. Agrawal, *Nonlinear Fiber Optics*, 2nd ed. (Academic Press, 1995), Chap. 3.
12. Mitsunobu Miyagi and Shigeo Nishida, "Pulse spreading in a single-mode fiber due to third-order dispersion," *Appl. Opt.* **18**, 678-682 (1979).
13. Eric W. Weisstein, "Airy Functions," From *MathWorld*--A Wolfram Web Resource, <http://mathworld.wolfram.com/AiryFunctions.html>.

## 1. Introduction

Thin-film filters (TFFs) have been widely employed in wavelength-division-multiplexing (WDM) networks for their many attractive features, including simple design and high yield, very low temperature dependence, thus eliminating the need for temperature controllers, small insertion loss, and low polarization dependence [1]. However, unlike other types of filters such as arrayed waveguide gratings, the TFFs exhibit large dispersion slopes [2]. The performance of cascaded TFFs is of major importance as signals may pass through multiple TFFs before they are dropped at the destinations [3]. The previous studies include simulations [3,4] and experiments [5-7] investigating system penalties caused by the dispersion and passband characteristics of cascaded filters. However, these simulation or experimental works were limited to 10-Gb/s signals. At 40-Gb/s line rate, neither the performance evaluation for the cascaded TFFs nor the analytical explanation of the TFF performance has been provided. Due to the wide spectral widths of 40-Gb/s signals, the dispersion slope and passband shape of the TFFs dominate the system penalty. Therefore the analytical method would be fundamentally different from those for lower rate scenarios, where the signal distortion induced by the in-band dispersion slope is not obvious.

In this paper we investigate the system performance of 40-Gb/s return-to-zero (RZ) signals passing through a number of cascaded TFFs with 100-GHz channel spacing. We perform simulations to study how the eye closure penalties vary with the number of cascaded filters, as well as the amount of frequency offset between the signal and the filter. Results show that the filtering effects of the TFFs can compensate the system degradation caused by the dispersion slope. Furthermore, the eye opening of the signal can be improved by properly detuning the signal frequency. We develop a theoretical model to explain and understand these observations. The model reveals that the ringing on the falling edge of the pulse caused by the dispersion slope can be decreased by applying bandwidth limitation. In addition, the residual inter-symbol interference (ISI) can be further reduced by the signal-filter offset, which introduces certain phase shift between adjacent pulses.

The theoretical model derived in this paper in general applies when dispersion slope and filtering effects play important roles. For example, in ultra-high-speed ( $>40$  Gb/s) long-haul WDM networks where large fiber dispersion slope is accumulated, optical add-drop multiplexers (OADMs) or optical cross-connects (OXC)s can be properly designed based on the developed model to mitigate the impairment. The model can also be used to analyze the distortion of filtered ultra-short optical pulses in the presence of 3<sup>rd</sup> order dispersion. Therefore, the model provides an alternative to specially designed filters for dispersion-slope compensation [8] by choosing an optimum readily available band-pass filter.

## 2. Simulation of 40-Gb/s RZ signals through cascaded TFFs

The impact of dispersion and passband characteristics of cascaded TFFs is investigated for 40-Gb/s RZ signals with a 50% duty cycle. The system model includes a transmitter, a transmission link consisting of cascaded 100-GHz TFFs, and an ideal photo detector.

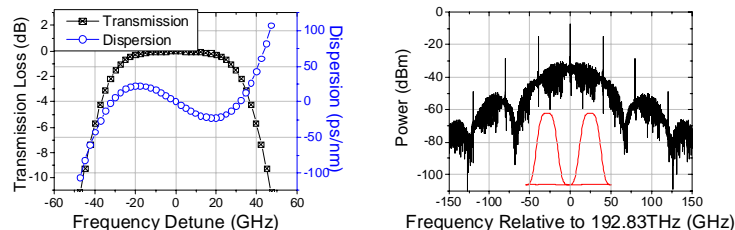


Fig. 1. (a) Measured transmission and dispersion characteristics of the TFF, and (b) Spectra and eye diagram of RZ signals.

The transmission and dispersion characteristics of the TFF are obtained by fitting the experimentally measured data of a prototype TFF (Fig. 1(a)). A  $2^{11}-1$  pseudorandom bit sequence (PRBS) is used as the signal pattern. The eye diagram and spectra of the RZ signals are shown in Fig. 1(b). The eye closure penalty (ECP) measured with a rectangular window having a 20% bit-width is used to quantify the performance of the received signals. It should be noted that numerous factors such as chirp of the laser source, bandwidth of the receiver [9], amplified spontaneous emission noise [7], polarization mode dispersion, polarization dependent loss, etc., may affect the system performance in a real experiment. Numerical modeling of all the above factors has been known to be a challenge. On the other hand, insights on the impact of individual devices or subsystems, which are relatively difficult to obtain in a transmission experiment, can be beneficial in the process of system design. Therefore, in our analytical and numerical approaches, we mainly focus on the dispersion slope and the filtering effects of the cascaded TFFs so that the underlying physical mechanisms can be revealed.

Figure 2(a) shows the ECPs caused by both the dispersion slope and passband shape of the cascaded TFFs. To isolate the impact of the dispersion characteristics of the TFFs, the penalties induced only by the dispersion are also provided, as shown in Fig. 2(b). For both cases, the effects of frequency detuning between the signals and the filters are illustrated.

A comparison between Fig. 2(a) and Fig. 2(b) leads to an interesting observation: when the number of the cascaded TFFs is rather large (7 in this study), which corresponds to a large accumulated dispersion slope of  $875 \text{ ps/nm}^2$ , the filtering effects of the TFFs behave favorably by helping reduce the ECPs caused by the dispersion slope. In the case of 7 TFFs cascaded, the ECP reduction is as much as 2 dB.

It is equally worth noting that minimal ECPs are obtained at nonzero frequency detune between the signals and the TFFs in both Fig. 2(a) and Fig. 2(b). Specifically in Fig. 2(a), the ECP minima occur at the frequency detune of  $\pm 10 \text{ GHz}$ . The eye diagrams in the insets of Fig. 2(a) agree with the ECP values and suggest that the ISI is reduced by the signal-filter offset. Simulation was also carried out to take into account the bandwidth limitation of a conventional receiver, which is typically 0.7 times of the bit rate. The general trends of the ECPs follow the ones shown in Fig. 2.

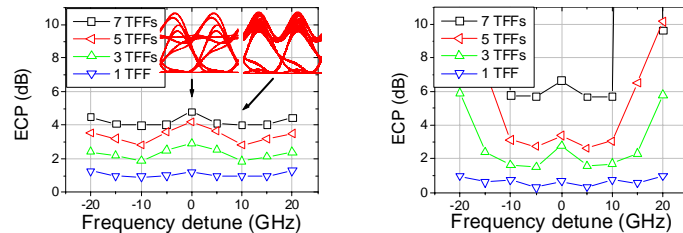


Fig. 2. (a) ECPs caused by both dispersion characteristics and passband shape of the TFFs, and (b) ECPs caused by dispersion characteristics of the TFFs only.

In the following we provide an analytical study to reveal the mechanisms behind the observations. For simplicity, we model the signals and filters using Gaussian approximations and explain the pulse behaviors and interactions for typical bit patterns. Note that although the filter shape given in Fig. 1(a) is more flat-top than Gaussian, the equivalent filter passband becomes close to Gaussian shape when the number of cascaded TFFs is large. Moreover, it turns out that a Gaussian approximation greatly simplifies our analysis and enables the understanding of the physical principles.

### 3. Analytical explanation

Since the dispersion tolerance for 40-Gb/s RZ signals with a duty cycle of 50% is  $61 \text{ ps/nm}$  at a power penalty of 1 dB [10], the accumulated dispersion within the frequency-detune range of interest in Fig. 2 is not expected to be a dominant impairment, thus the penalty in Fig. 2(b) mainly comes from the dispersion slope. To facilitate theoretical derivation, we treat the TFF as a series combination of an ideal Gaussian filter and a dispersive component. We then

consider an ideal Gaussian pulse entering a Gaussian filter followed by a dispersive component with large dispersion slope. The bit period of the Gaussian pulses is 25 ps corresponding to 40-Gb/s bit rate.

The field of a modulated optical pulse can be expressed as

$$E(t) = A_0 \exp\left[-t^2/(2\tau^2) - i(\omega_0 + 2\pi\Delta f)t\right] \quad (1)$$

where  $A_0$  is either 0 or 1 for on-off keying (OOK) modulation,  $\tau$  is the pulse's half-width at  $1/e$ -intensity profile,  $\Delta f$  is the signal detune from the filter's central frequency, and  $\omega_0 + 2\pi\Delta f$  is the angular frequency of the laser.

The response function of an ideal Gaussian optical filter in the frequency domain can be given by

$$R_1(\omega) = \exp\left[-(\omega - \omega_0)^2/(2\sigma^2)\right] \quad (2)$$

where  $\omega_0$  is the angular frequency corresponding to the central frequency of the Gaussian filter, and  $\sigma$  is related to the filter's 3-dB bandwidth  $\Delta f_{3dB}$  (in Hz) through  $\Delta f_{3dB} = \sigma\sqrt{\ln 2}/\pi$ .

For a component with an accumulated dispersion slope of  $DS$  (in ps/nm<sup>2</sup>) and zero dispersion at  $\omega_0$ , its response function [11,12] across the bandwidth of our interest can be described as

$$R_2(\omega) = \exp[i\varphi(\omega)] = \exp\left[i2\pi^2c^2DS(\omega - \omega_0)^3/3\omega_0^4\right] \quad (3)$$

The field of the Gaussian pulse going through the Gaussian filter and the dispersive component described above can be calculated analytically, i. e.:

$$E'(t) = \frac{\sqrt{2\pi}A_0\tau}{2\pi} \exp(-i\omega_0 t) \times \int_{-\infty}^{\infty} \exp\left[-B(\omega - \omega_0)^2\right] \exp\left[i\frac{A(\omega - \omega_0)^3}{3}\right] \times \exp\left[2\pi\Delta f(\omega - \omega_0)\tau^2 - 2\pi^2\Delta f^2\tau^2\right] \exp[-i(\omega - \omega_0)t] d\omega \quad (4)$$

where

$$A = 2\pi^2c^2DS/\omega_0^4, \text{ and } B = (\tau^2 + 1/\sigma^2)/2 \quad (5)$$

By substituting the variable  $\omega$  and noting that  $\omega = \omega_1/\sqrt[3]{A} - iB/A + \omega_0$ , Eq. (4) can be rewritten as

$$\begin{aligned} E'(t) &= \frac{\sqrt{2\pi}A_0\tau}{\sqrt[3]{A}} \exp\left[-i\omega_0 t - \frac{B}{A}t + \frac{2B^3}{3A^2} - i\frac{B2\pi\Delta f\tau^2}{A} - 2\pi^2\Delta f^2\tau^2\right] \\ &\times \frac{1}{2\pi} \int_{-\infty}^{\infty} \exp\left[i\frac{\omega_1^3}{3} + \frac{i}{\sqrt[3]{A}}\left(\frac{B^2}{A} - i2\pi\Delta f\tau^2 - t\right)\omega_1\right] d\omega_1 \quad (6) \\ &= \frac{\sqrt{2\pi}A_0\tau}{\sqrt[3]{A}} \exp\left[-i\omega_0 t - i\frac{B2\pi\Delta f\tau^2}{A}\right] \exp\left[-\frac{B}{A}t + \frac{2B^3}{3A^2} - 2\pi^2\Delta f^2\tau^2\right] \\ &\times Ai\left(\frac{B^2 - At - iA2\pi\Delta f\tau^2}{A\sqrt[3]{A}}\right) \end{aligned}$$

where  $Ai(z)$  is the Airy function defined as  $Ai(z) = 1/2\pi \times \int_{-\infty}^{\infty} \exp[i(zx + x^3/3)] dx$ . The Airy function with real independent variable is also a real function and its behavior [12] is shown in Fig.3. The first few real roots for  $Ai(z)$  to reach zero are approximately -2.338, -4.088, -5.521 and -6.787 [13].

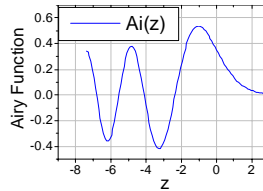


Fig. 3. Behavior of the Airy function  $Ai(z)$  with real independent variable.

If the frequency offset between the signals and the center of the filter is set to zero, Eq. (6) can be simplified to

$$E'(t) = \sqrt{2\pi}A_0\tau/\sqrt[3]{A} \times \exp(-i\omega_0 t) \exp(-Bt/A + 2B^3/3A^2) \times \text{Ai}((B^2 - At)/A\sqrt[3]{A}) \quad (7)$$

Equation (7) shows that the pulse shape is distorted and becomes asymmetric with an oscillatory structure near its falling edge, due to the dispersion slope of concern [11,12].

To show the effect of dispersion slope on pulse interactions, we consider two consecutive Gaussian pulses with a duty cycle of 50% at 40 Gb/s that are subject to an accumulated dispersion slope of 875 ps/nm<sup>2</sup>. Figure 4(a) depicts the normalized total field of the output pulses in the temporal domain, in which T is the bit period and the dashed lines in black represent the fields of the isolated optical pulses. Due to the oscillatory feature of the Airy function, the field of an optical pulse becomes negative when the values of  $(B^2 - At)/A\sqrt[3]{A}$  range from -2.338 to -4.088. Correspondingly, the values of  $t$  are between 22 ps and 37 ps, which happen to fall in the next bit slot. Consider bit pattern "110", where the tail of the first "1" pulse interferes destructively with the second "1" pulse, lowering the "1" level. Moreover, the oscillation on the tail of the second "1" pulse extends well into the "0" bit, lifting the "0" level. Both effects contribute to the closure of the eye.

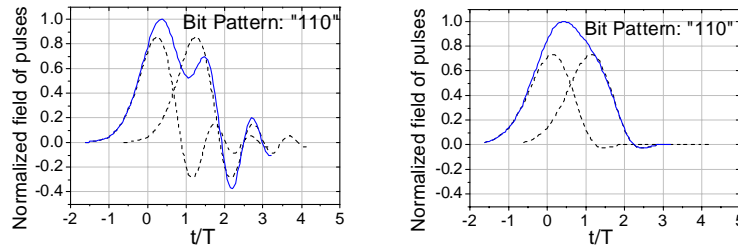


Fig. 4. Normalized total field of two consecutive optical pulses subject to (a) DS of 875 ps/nm<sup>2</sup>, and (b) DS of 875 ps/nm<sup>2</sup> and 7 cascaded Gaussian filters. T represents the bit period.

However, if Gaussian filters are applied, it can be seen from Eq. (5.2) that parameter  $B$  becomes larger, which results in two effects that are inherently correlated: firstly the value of  $t$  for the pulse field to reach zero is increased, and secondly, the oscillations near the falling edges of the pulses are reduced. Therefore, the destructive interference with the neighboring pulse is significantly mitigated by the filtering effect. Figure 4b shows the normalized field of optical pulses after passing through a dispersive component with a dispersion slope of 875 ps/nm<sup>2</sup> and 7 Gaussian filters. The 3-dB bandwidth of each Gaussian filter is 65 GHz. For the same bit pattern "110", the interference between the two consecutive "1" pulses now almost becomes constructive, without lowering the "1" level. In the meanwhile, the oscillation in the "0" bit slot is greatly suppressed. Although the pulses are broadened due to the filtering effects of the Gaussian filters, as can be seen in Fig. 4(b), the eye remains open owing to the reduced ISI. The above analysis suggests that the fine features on the pulse edges can play an important role, and in some cases their impact can be more significant than that caused by pulse broadening.

Considering nonzero frequency detune between the signals and the central frequencies of the filters (as expressed in Eq. (6)), the independent variable in the Airy function becomes complex, and the Airy function in Eq. (6) also becomes a complex function that contains both amplitude and phase information. It turns out that the exact explanation about the combined effects of dispersion slope and detuned Gaussian filtering is too complicated to provide. We therefore use examples to explain such effects in the following.

We now consider the bit pattern "101". The normalized amplitudes and phases of the pulses after experiencing a dispersion slope and cascaded Gaussian filtering without and with frequency detune are shown in Fig. 5(a) and Fig. 5(b), respectively. The phases of the optical pulses are represented with the red solid lines, the dashed lines in black denote the fields of the isolated optical pulses, and, as before, the blue solid lines depict the total field of the bit pattern. The parameters of the dispersive components and Gaussian filters are the same as

those used in the previous examples. In our analysis we also performed simulations for other patterns, and it turned out that the “110” pattern without filtering and the “101” pattern in the presence of filtering but without frequency detune are the critical ones of major concern. Therefore we focus on these two exemplary cases in the study.

In Fig. 5(a) the phase is zero across the optical pulses. Therefore, the tails of the “1” pulses interfere constructively in the “0” bit slot, elevating the “0” level and causing the eye to close. However, when certain frequency detune between the signals and filters is applied, the phase across a pulse is no longer constant and varies with time. For small frequency detune, the real part of the Airy function in Eq. (6) contributes more to the pulse shape than its imaginary part, and the phase decreases gradually with time before the pulse field diminishes, as shown in Fig. 5(b). For the bit pattern “101”, the additive interference between the tails of the “1” bits that can lift the “0” level shown in Fig. 5(a) now can be partially reduced due to the phase difference between the two “1” bits. Compared to Fig. 5(a), the eye opening of the signals is improved through proper detuning of the signal.

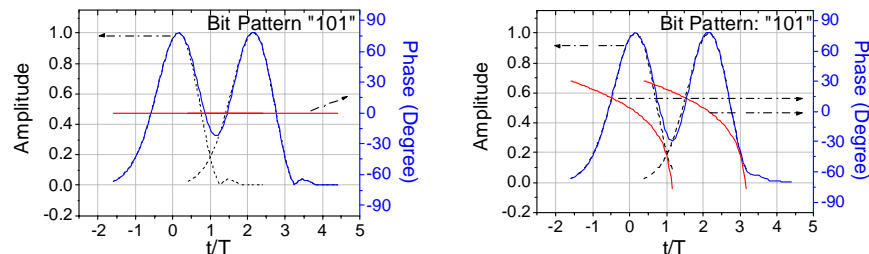


Fig. 5. Normalized amplitudes and phases of optical pulses subject to a dispersion slope of  $875\text{ps}/\text{nm}^2$  and 7 cascaded Gaussian filters (a) without detune, and (b) with 10-GHz detune.

It has been shown recently that the phase variation introduced by the vestigial sideband (VSB) filtering could reduce the ISI due to the destructive interference between the neighboring bits [14]. In that work, the theoretical model is limited to Gaussian filters, and, as a result, the filtered pulse maintains a Gaussian shape and its phase varies linearly with time. In our analysis, the dispersion slope of the TFFs needs to be taken into account as well due to its dominating impact, which results in properties and interactions of the filtered pulses that are different from those discussed in [14]. Due to the complexity introduced by the dispersion slope, the filtered pulse can no longer be described with a Gaussian approximation and instead the Airy function has to be introduced in our theoretical model. The Airy function dictates that the phase across the pulse decreases more dramatically with time than a linear descent, thus resulting in effective ISI suppression under certain conditions.

#### 4. Conclusion

We have investigated the performance of cascaded TFFs in optical communication systems operating at 40 Gb/s. Simulations are carried out for RZ signals through cascaded TFFs with 100-GHz channel spacing, where the dispersion slope is the main source of penalties. An analytical model is established to reveal the underlying principle of the combined effects of dispersion slope and filtering. Both the simulation results and theoretical analysis show that the penalty caused by large dispersion slope can be alleviated by the filtering effects and that further performance improvement can be achieved by properly detuning the signal frequency with respect to the TFFs. The theoretical model in this paper may also find applications in high-speed long-haul OADM/OXC networks with large accumulated fiber dispersion slope and ultra-fast systems employing very short optical pulses.

#### Acknowledgments

This work was supported by the National Natural Science Foundation of China under the grants 60407008/60407010/90304002, Shanghai Optical Science and Technology grants 012261030/04dz05103, Shanghai rising star program 04QMX1413, and Li foundation.